Environ Sci Pollut Res (2014) 21:1514–1527
DOI 10.1007/s11356-013-2035-9

RESEARCH ARTICLE

Use of a reactive transport model to describe reductive dechlorination (RD) as a remediation design tool: application at a CAH-contaminated site

Paolo Viotti · Paolo Roberto Di Palma · Federico Aulenta · Antonella Luciano · Giuseppe Mancini · Marco Petrangeli Papini

Received: 23 February 2013 / Accepted: 22 July 2013 / Published online: 10 August 2013

Abstract In this paper, a numerical model is presented that is capable of describing the complex set of biochemical processes that occur in chlorinated aliphatic hydrocarbon (CAH)-contaminated groundwater when an exogenous electron donor is added. The reactive pattern is based on the degradation pathways of both chlorinated ethanes and ethenes, and it includes electron donor production (H_2 and acetate) from the fermentation of an organic substrate as well as rate-limiting processes related to electron acceptor competition. Coupling of the kinetic model to a convection–dispersion module is described. The calibration phase was carried out using data obtained at a real CAH-contaminated site in the north of Italy. Model simulations of different application scenarios are presented to draw general conclusions on the effectiveness of reductive dechlorination (RD) as a possible cleanup strategy. Early outcomes indicate that cleanup targets can only be achieved if source longevity is reduced. Therefore, metabolic RD is expected to produce beneficial effects because it is known to induce bioenhanced degradation and transformation of CAHs.

Keywords Reductive dechlorination · Reactive transport model · Chlorinated ethenes · Chlorinated ethanes

Responsible editor: Michael Matthies

P. Viotti (✉) · P. R. Di Palma
Department of Civil, Building and Environmental Engineering, Sapienza University of Rome, Via Eudossiana 18, 00184 Rome, Italy
e-mail: paolo.viotti@uniroma1.it

F. Aulenta
IRSA-CNR Water Research Institute-National Research Council, Via Salaria km 29.300, Monterotondo, Rome, Italy

A. Luciano
ENEA Italian National Agency for New Technologies, Energy and Sustainable Economic Development, RC Casaccia, Via Anguillarese 301, S. Maria Galeria, 00123 Rome, Italy

G. Mancini
Department of Industrial Engineering, University of Catania, Viale Andrea Doria 6, 95125 Catania, Italy

M. P. Papini
Department of Chemistry, Sapienza University of Rome, P.le aldo Moro 5, 00185 Rome, Italy

Introduction

Groundwater (GW) contamination, caused by the release and dispersion of chlorinated aliphatic hydrocarbons (CAHs) in the subsurface, is a common problem at many industrial sites and poses serious threats to human health and the environment. In subsurface environments, CAHs are often present in the form of dense nonaqueous phase liquids (DNAPLs), which act as long-term sources of contamination by slowly dissolving into the GW (Rivett et al. 2001; Roy et al. 2002). Under natural conditions, the dissolution of DNAPLs and the release of CAHs may require hundreds of years to complete. Given the intrinsic difficulties in the characterization of DNAPL sources, their removal is often incomplete and residual DNAPL pools continue to release CAHs for a long time (Roy et al. 2002). This necessitates the containment and treatment of CAH plumes for an equally long time. Pump and treat (P&T), which consists of the interception of an entire contaminated plume, extraction of the contaminated GW, and treatment by on-site facilities, is one of the most widely applied technologies for plume management. Although P&T effectively reduces the risk of contaminant transport away from the source area, it has the serious drawback of high operating costs due to both the high energy demand required to pump out large volumes of GW and the high GW treatment

costs (often related to the use of activated carbon as an adsorbent material for CAHs). Moreover, by treating only the dissolved fraction of the contaminants, the P&T approach does not usually reduce the longevity of the DNAPL sources.

To overcome these problems, different approaches for the removal of contaminants from a source area and for the sustainable management of contaminated plumes have been proposed in recent years. Regarding contaminant removal or destruction near source zones, several technologies have been proposed, including chemical oxidation or reduction, flushing, thermal treatment, anaerobic bioremediation (Boulding et al. 2004) and injection of zerovalent iron (Tosco et al. 2012). With respect to plume management, in situ biological reduction of CAHs seems to be a valid approach that is capable of overcoming most of the limitations associated with P&T. The in situ approach is accomplished by injecting an exogenous electron donor into the GW to stimulate endogenous bacteria to use CAHs as electron acceptors, a metabolic process often referred to as reductive dechlorination (RD) (Fennell and Gossett 1998; Wiedemier et al. 1999; Fennel et al. 2001; Suthersan 2002). Considering that most dechlorinating bacteria use H_2 as the actual electron donor, the primary function of the injected electron donor is to release H_2 through fermentation reactions (Logan et al. 2002).

Despite promising laboratory evidence, full-scale application of this relatively simple process is still quite limited (Clement et al. 1998; Witt et al. 2000; Clement et al. 2001; Nobre and Nobre 2004; Wood 2005; Kuchovsky et al. 2007) because a proper understanding of its dynamics in the subsurface is necessary to both control the process and have it authorized. Furthermore, an accurate computation of electron donor dosage and the selection of an optimal addition strategy have been found to be strongly site specific. Thus, scaling-up this technology from the laboratory to the field requires tools capable of fully representing what happens when an electron donor is added to the GW to stimulate RD processes.

Some kinetic models have already been proposed (Fennell and Gossett 1998; Bagley 1998), but none of them consider the whole set of possible degradative pathways, H_2-releasing fermentative reactions, and H_2-consuming competitive processes. Furthermore, such models generally refer exclusively to the RD of chlorinated ethenes and not that of chloroethanes, which are also common GW contaminants.

Therefore, in this work, a specific reaction module has been developed to account for both chlorinated ethane and ethene RD as well as for the RD-related processes mentioned above. The model has subsequently been coupled with a convection–dispersion (CD) module to allow for the simulation of process enhancement at full scale.

Model development

Processes description

Several laboratory microcosm studies (Lorah and Voytek 2002; Aulenta et al. 2006a) have confirmed that there are multiple biotic and abiotic processes involved in the biological degradation of chlorinated ethanes and ethenes and that these should include at least the following:

- The fermentation of injected organic substrates (Aulenta et al. 2006b) (i.e., lactate, butyrate, yeast extract, etc.) and the resulting formation of H_2, which is the electron donor used by the majority of dechlorinating bacteria. Notably, certain substrates are degraded via alternative fermentation pathways, depending on the environmental conditions, such as the H_2 concentration. As an example, lactate can be converted to a mixture of either acetate and propionate (without H_2 formation) or acetate and H_2. The shift in the fermentation pathway is triggered by the H_2 concentration levels: production of H_2 and acetate is energetically favored at low H_2 concentrations (e.g., when the produced H_2 is rapidly consumed by dechlorinators or other H_2-utilizing bacteria); production of acetate and propionate is favored when H_2 accumulates at relatively high levels because of an imbalance between the rates of formation and consumption.
- The sequential (reductive) dechlorination of CAHs (e.g., chlorinated ethanes and ethenes) via multiple reaction pathways, such as hydrogenolysis, dichloroelimination, and abiotic dehydrochlorination. Notably, while hydrogenolysis and dichloroelimination are H_2-consuming reactions, dehydrochlorination is not a redox reaction and it does not require the input of H_2 to proceed. It is widely reported in the literature that certain dechlorinating bacteria can use, in addition to H_2, other electron donors, such as acetate, to dechlorinate CAHs. However because the majority of dechlorinating microorganisms preferentially use H_2 or are even restricted to using H_2 as an electron donor, only H_2-dependent RD reactions were considered in the model for reasons of simplicity. A scheme of the processes included in the model is displayed in Fig. 1.

Model description

The model takes into account the simulation of a large set of chemical species: 10 CAHs, the fermentable organic substrate and its fermentation by-products (i.e., H_2, methane, acetate, and propionate). The behavior of the by-products in a plume migrating downgradient of a source-zone is investigated by considering an equivalent number of nonstationary 2D reactive transport equations:

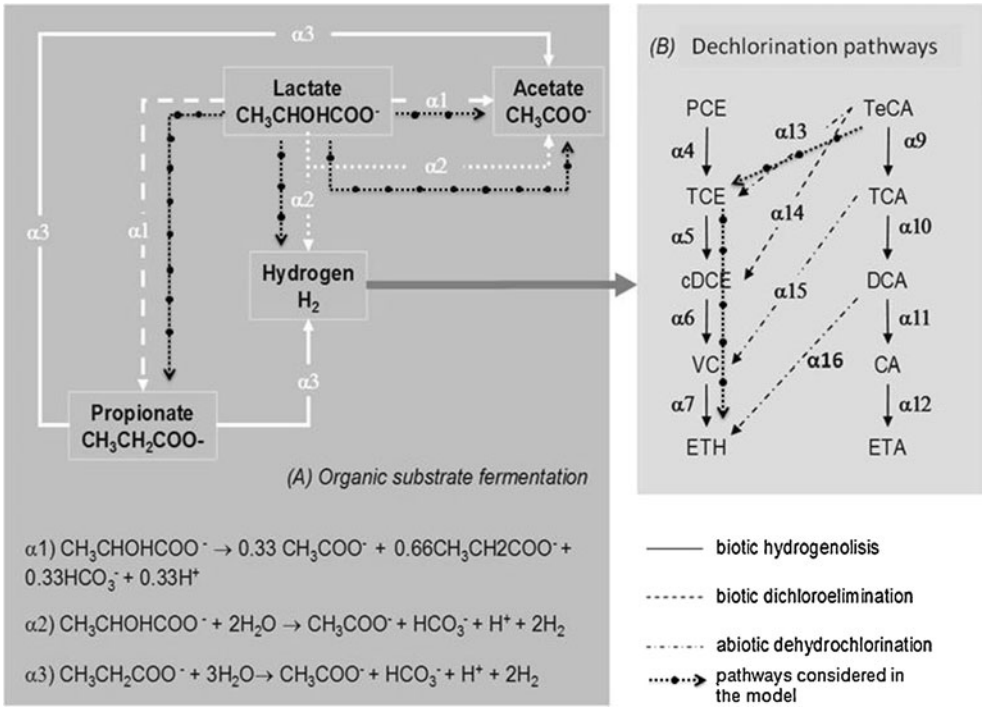

Fig. 1 Catabolic processes involved in electron donor (lactate) utilization and RD of chloroethanes and chloroethenes

Table 1 Rate expressions ($T_{i,k}$) for biotic and abiotic transformation processes

Number	Process	Rate expression
Organic substrate fermentation		
α_1	Lactate conversion into acetate and propionate	$k_{\mathrm{LatAc}} X_{\mathrm{LatAc}} \left(\frac{\mathrm{LAT}}{\mathrm{LAT}+K_{S_{\mathrm{LatAc}}}}\right)$
α_2	Lactate conversion into acetate and H_2, including inhibition due to high H_2 concentrations	$k_{\mathrm{LatH_2}} X_{\mathrm{LatH_2}} \left(\frac{\mathrm{LAT}}{\mathrm{LAT}+K_{S_{\mathrm{LatH_2}}}}\right)\left(\frac{K_{\mathrm{INL}}}{K_{\mathrm{INL}}+\mathrm{H_2}}\right)$
α_3	Propionate conversion into acetate and H_2, including inhibition due to high H_2 concentrations	$k_{\mathrm{ProH_2}} X_{\mathrm{ProH_2}} \left(\frac{\mathrm{PRO}}{\mathrm{PRO}+K_{S_{\mathrm{Pro}}}}\right)\left(\frac{K_{\mathrm{INPRO}}}{K_{\mathrm{INPRO}}+\mathrm{H_2}}\right)$
Reductive dechlorination of ethenes and ethanes		
α_4	Biological hydrogenolysis (PCE→TCE)	$k_{\mathrm{PCE}} X_{\mathrm{RD1}} \left(\frac{\mathrm{PCE}}{\mathrm{PCE}+K_{S_{\mathrm{PCE}}}}\right)\left(\frac{\mathrm{H_2}-\mathrm{H_2tr}}{\mathrm{H_2}-\mathrm{H_2tr}+K_S\mathrm{H_{PCE}}}\right)$
α_9	Biological hydrogenolysis (TeCA→TCA)	$k_{\mathrm{TeCA}} X_{\mathrm{RD1}} \left(\frac{\mathrm{TeCA}}{\mathrm{TeCA}+K_{S_{\mathrm{TeCA}}}}\right)\left(\frac{\mathrm{H_2}-\mathrm{H_2tr}}{\mathrm{H_2}-\mathrm{H_2tr}+K_S\mathrm{H_{TeCA}}}\right)$
α_{13}	Abiotic dehydrochlorination (TeCA→TCE)	k_{TeCATCE} TeCA
α_{14}	Biological dichloroelimination (TeCA→DCE)	$k_{\mathrm{DCETeCA}} X_{\mathrm{RD2}} \left(\frac{\mathrm{TeCA}}{\mathrm{TeCA}+K_{S_{\mathrm{TeCA}}}}\right)\left(\frac{\mathrm{H_2}-\mathrm{H_2tr}}{\mathrm{H_2}-\mathrm{H_2tr}+K_S\mathrm{H_{DCETeCA}}}\right)$
α_5	Biological hydrogenolysis (TCE→DCE)	$k_{\mathrm{TCE}} X_{\mathrm{RD2}} \left(\frac{\mathrm{TCE}}{\mathrm{TCE}+K_{S_{\mathrm{TCE}}}}\right)\left(\frac{\mathrm{H_2}-\mathrm{H_2tr}}{\mathrm{H_2}-\mathrm{H_2tr}+K_S\mathrm{H_{TCE}}}\right)$
α_6	Biological hydrogenolysis (DCE→VC)	$k_{\mathrm{DCE}} X_{\mathrm{RD2}} \left(\frac{\mathrm{DCE}}{\mathrm{DCE}+K_{S_{\mathrm{DCE}}}}\right)\left(\frac{\mathrm{H_2}-\mathrm{H_2tr}}{\mathrm{H_2}-\mathrm{H_2tr}+K_S\mathrm{H_{DCE}}}\right)$
α_{10}	Biological hydrogenolysis (TCA→DCA)	$k_{\mathrm{TCA}} X_{\mathrm{RD2}} \left(\frac{\mathrm{TCA}}{\mathrm{TCA}+K_{S_{\mathrm{TCA}}}}\right)\left(\frac{\mathrm{H_2}-\mathrm{H_2tr}}{\mathrm{H_2}-\mathrm{H_2tr}+K_S\mathrm{H_{TCA}}}\right)$

Table 1 (continued)

Number	Process	Rate expression
α_{15}	Biological hydrogenolysis (TCA→VC)	$k_{\mathrm{VCTCA}} X_{\mathrm{RD2}} \left(\frac{\mathrm{TCA}}{\mathrm{TCA}+K_{S_{\mathrm{VCTCA}}}}\right)\left(\frac{\mathrm{H_2-H_2tr}}{\mathrm{H_2-H_2tr}+K_S \mathrm{H_{VCTCA}}}\right)$
α_7	Biological hydrogenolysis, including inhibition due to the presence of highly chlorinated CAHs (VC→ETH)	$k_{\mathrm{VC}} X_{\mathrm{RD2}} \left(\frac{\mathrm{VC}}{\mathrm{VC}+K_{S_{\mathrm{VC}}}\left(1+\frac{\mathrm{PCE}}{K_{S\mathrm{PCE}}}+\frac{\mathrm{TCE}}{K_{S\mathrm{TCE}}}+\frac{\mathrm{DCE}}{K_{S\mathrm{DCE}}}\right)}\right)\left(\frac{\mathrm{H_2-H_2tr}}{\mathrm{H_2-H_2tr}+K_S \mathrm{H_{VC}}}\right)$
α_{11}	Biological hydrogenolysis (DCA→CA)	$k_{\mathrm{DCA}} X_{\mathrm{RD2}} \left(\frac{\mathrm{DCA}}{\mathrm{DCA}+K_{S_{\mathrm{DCA}}}}\right)\left(\frac{\mathrm{H_2-H_2tr}}{\mathrm{H_2-H_2tr}+K_S \mathrm{H_{DCA}}}\right)$
α_{12}	Biological hydrogenolysis (CA→ETA)	$k_{\mathrm{CA}} X_{\mathrm{RD2}} \left(\frac{\mathrm{CA}}{\mathrm{CA}+K_{S_{\mathrm{CA}}}}\right)\left(\frac{\mathrm{H_2-H_2tr}}{\mathrm{H_2-H_2tr}+K_S \mathrm{H_{CA}}}\right)$

$$R\frac{\partial C_i}{\partial t} = \frac{\partial}{\partial x}\left(D_x \frac{\partial C_i}{\partial x}\right) + \frac{\partial}{\partial y}\left(D_y \frac{\partial C_i}{\partial y}\right) - v_x \frac{\partial C_i}{\partial x} - v_y \frac{\partial C_i}{\partial y} \pm \sum_k \gamma_{i,k} T_{i,k}$$

where: x_i, y_i are the spatial coordinates (i, j=1, 2; L); C_k is the concentration of each chemical species in the water (k=1.19; $M \cdot L^{-3}$); D_i are the components of the hydrodynamic dispersion tensor ($L^2\ T^{-1}$); v_i are the components of the velocity vector ($L\ T^{-1}$); R_i is the retardation factor; $T_{i,k}$ is the transformation rate ($M\ L^{-3}\ T^{-1}$); $\gamma_{i,k}$ are the stoichiometric coefficients.

As shown in Table 1, each component transformation (i.e., production and degradation) is described by Monod-like kinetic expressions that are modified to incorporate electron donor thresholds (H_2thr) (Fennell and Gossett 2003), which represent the lowest aqueous H_2 concentrations that dechlorinating microorganisms are able to use. A number of studies have shown that H_2 thresholds linked to metabolic RD fall within the range 0.04–0.3 nM and are almost independent of the chlorinated compound being used (Löffler et al. 1999). As for the hydrogenolysis of VC (reaction α7 in Fig. 1), competitive inhibition of more chlorinated ethenes (PCE, TCE, and DCE) was assumed (Bagley 1998; Yu et al. 2005).

Two different bacterial populations of dechlorinating microorganisms were considered, one being responsible for the RD of chloroethanes (via hydrogenolysis and dichloroelimination) and more chlorinated ethenes (PCE and TCE) and the second being responsible for the RD of *cis*-DCE and VC. This assumption reflects the fact that bacteria capable of chloroethane dechlorination (e.g., *Dehalobacter* spp. and *Desulfitobacterium* spp.) are, in most cases, also capable of partial PCE dechlorination (via hydrogenolysis) to TCE and *cis*-DCE (Grostern and Edwards 2006; Rossetti et al. 2008). Conversely, *Dehalococcoides spp.* is the only known microorganism capable of dechlorinating DCE and VC; as a result of this capacity, it was identified as a separate population. For the transformation of TeCA into TCE, an abiotic dehydrochlorination (α13) was considered.

As a first approximation, biomass growth has been neglected by assuming that the concentration of the different microbial populations involved in the processes remained constant. A 2D flow field, generated with conventional MODFLOW-based simulators (Harbaugh et al. 2000) and given proper boundary conditions was used for the velocity field in the model.

Model application

Site description

Geology and hydrogeology of the Rho site

Numerical modeling was applied at a site in northern Italy, located in the Rho Municipality (Milan, Italy), where a former chemical facility, mostly involved in the production of synthetic dyes, was identified as the likely source of a large chlorinated solvent plume, extending over an area of approximately 0.4 km^2. Alluvial and fluvio-glacial Quaternary sediments geologically characterize the Municipality of Rho, which is located in the Lombard plain. The hydrogeological series of the aquifer allows the identification of two main superimposed water surfaces separated by a clay–loam horizon, which tends to increase its thickness with depth. These aquifers are portrayed as the shallow or first aquifer, second aquifer and deep aquifer. The first aquifer is composed mainly of gravel with a sandy matrix and the presence of limited and

isolated silty-clay lenses. This is separated from the second aquifer by an aquitard horizon, consisting of silt and clayed silt. The second aquifer is found in the fluvio-glacial deposits, mainly consisting of sand and gravel that is mostly cemented in addition to some clay.

Site history

The contamination plume most likely originated from the loss of a storage basin, where chlorinated solvents were discharged during the period of industrial activity of the "Chimica Bianchi." In 1982, local authorities carried out an emergency action consisting of the physical isolation of the area previously occupied by the storage tank with a lateral and surface concrete barrier. The encapsulation system was inserted into a thin layer of clay (approximately 1 m thick) separating the first aquifer (extending from 5 to 12 a.m.s.l.) from the second one (13 to 40 a.m.s.l.). This action was not completely successful due to discontinuities in the clay layer, resulting in contamination of the second aquifer. Monitoring the two aquifers downgradient from the area of contamination over the last 15 years has shown the stable presence of high concentrations of chlorinated solvents (up to 180 mg/L of trichloroethylene (TCE) and 50 mg/L of 1,1,2,2-tetrachloroethane (TeCA)) in the second aquifer, whereas the first one has shown very low concentrations of chlorinated compounds. The data from the site characterization and GW monitoring are consistent with a scenario in which the released contaminants were transported as DNAPLs from the underground storage tank through the thin clay layer down into the deep aquifer, where they are still present as DNAPL pools, ganglia, or residuals that act as long-term sources of contamination (Aulenta et al. 2007).

Since 1998, in the so-called Chimica Bianchi area, a series of monitoring campaigns have been conducted to control the evolution of contamination plumes (Fig. 2 shows the monitoring network). Multiple sampling techniques (e.g., multipacker, membrane interface probe) were used to characterize the area and its contamination status and evolution. Historical analysis of the concentration of total organohalogenated compounds has shown that, up to the year 2000, the maximum recorded concentrations were detected inside the area occupied by the original tank used as the final disposal system during the activity period, whereas higher concentrations were detected thereafter in piezometers located downgradient from the original source.

Calibration and results

The origin of the contamination source was hypothesized by considering the results obtained from prior investigation campaigns and information about industrial activities conducted at the site. The model was first calibrated using a set of available analytical data.

The domain used in the numerical simulation is shown in Fig. 3. The total extent of the investigated area is 1,325×1,255 m. The adopted discretization was based on a quadratic mesh (Dx=-Dy=10 m, three layers).

Application of the GW field model and of the reactive transport model

The velocity fields of the GW in the shallow (first layer) aquifer (Fig. 3) and in the deep (third layer) aquifer were obtained through the use of MODFLOW software (Beretta et. al. 2006; Bozzano et al. 2007) with a full 3D approach. Boundary conditions used for flow were in the form of constant head boundaries (first and third layers) that were determined from the head values of the water table measured in the observation wells. Figure 4 reports the results of the calibration phase for the GW velocity field. The Modflow model is decoupled from the transport model, thus its results are only used for the GW flow field.

The transport reactive model was applied in a 2D version being the contamination present only in the deep aquifer. This evidence stems from the velocity field analysis that has shown that downgradient from the source the aquitard was acting like an impermeable layer resulting in an independent behavior for the two aquifers. Therefore, the resulting 2D velocity field of the deep aquifer (third layer) was used as input to the authors' reactive transport model. For the boundary conditions of the reactive transport model, a null gradient was adopted for the integration domain limits and a constant concentration was assumed for the contamination source. TeCA and TCE concentration values from a field campaign in 2004 were chosen as the initial conditions for the transport model.

Calibration phase

The set of available data concerning the temporal and spatial distribution of CAHs were used for the preliminary calibration phase of the model, which was aimed at examining the effects exerted by source characteristics and location. Analysis of the available data appeared to indicate the presence of a persistent DNAPL pool acting as a long-term source of contamination, therefore suggesting the hypothesis of displacement of the non-miscible phase from the encapsulated source. Numerical simulations were carried out to confirm this preliminary evidence by comparing the case of a lack of an active source with one where a persistent source was located in the domain (in particular, a source close to the well is where the highest contaminant concentrations were observed (well 346)). Specifically, the interpolated spatial distribution of aqueous phase

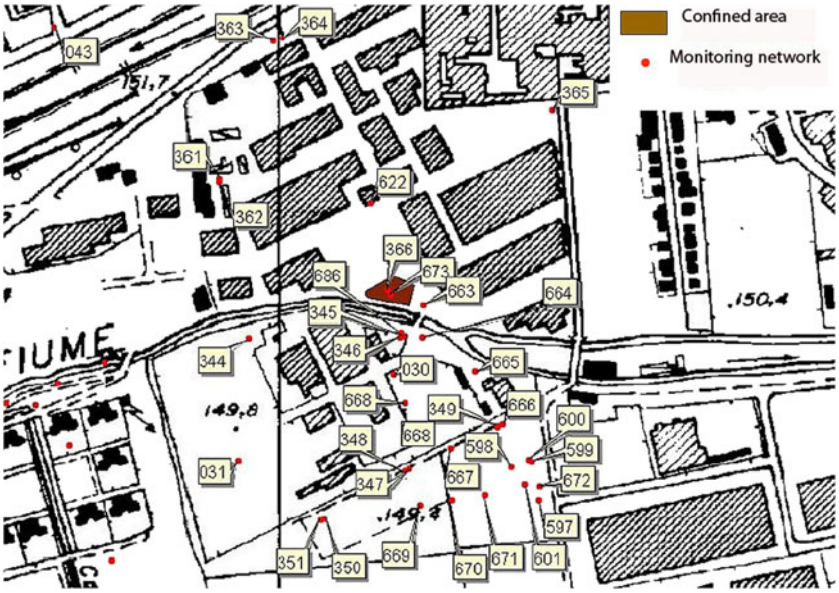

Fig. 2 Monitoring network implemented over the years at the site

TeCA and TCE concentrations, observed in the monitoring campaign of March 2003 on the existing network of wells, was set as the T_0 distribution of the contaminants of concern. Then, their evolution over space and time was simulated for a set of different source conditions. To evaluate the consistency of the formulated assumptions, the results from the model were compared with a later sampling campaign on the same network of wells (April 2004, T_1=9,600 h), as shown in Fig. 5a, b. A comparison between the observed TeCA and TCE concentrations with those simulated for a persistent source and for an exhausted source are presented in Fig. 6a–d.

As expected, the results of the model simulations do not support the absence of an active release of contaminants, as shown by the calculated values of the mean squared errors (MSE) for both TCE (Fig. 7a) and TeCA (Fig. 7b), which were 61.52 and 53.31 %, respectively. A significant reduction in the calculated errors was obtained when an active source was considered (MSE_{TCE}=18.75 % and MSE_{TeCA}=13.14 %)

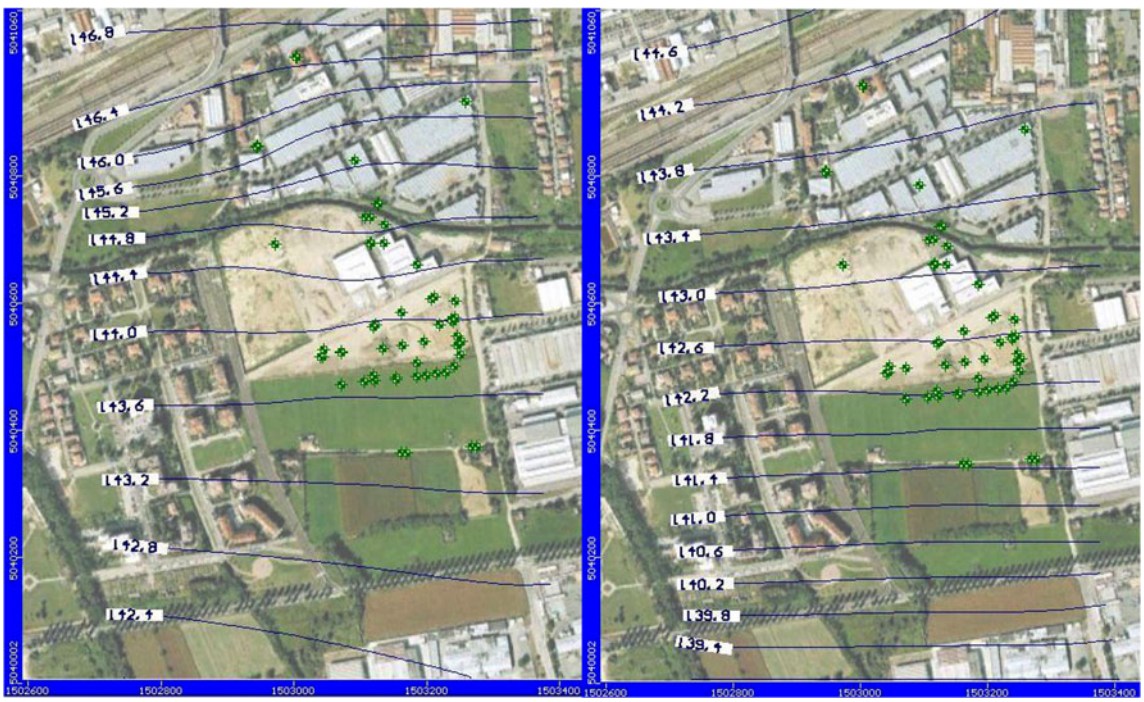

Fig. 3 Rebuilt GW velocity field in the aquifers at the investigated site

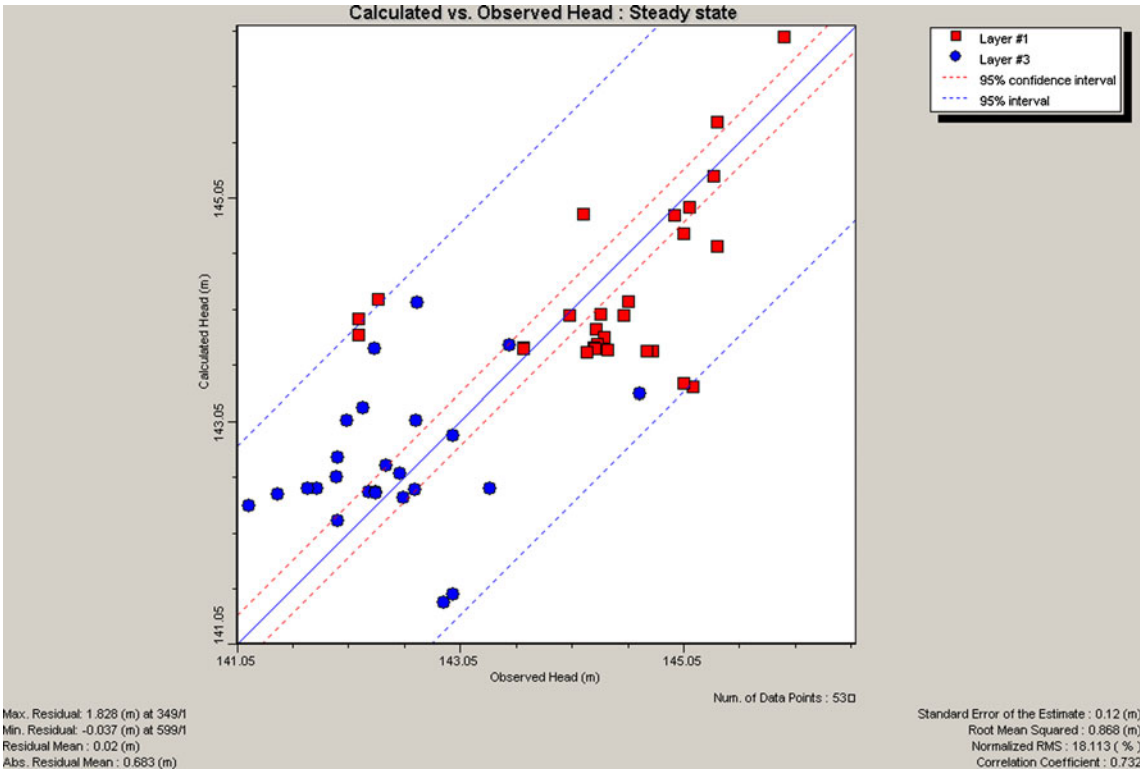

Fig. 4 Results of the calibration phase for the GW velocity field by VISUAL MODFLOW analysis

(Fig. 7c, d). This reduction in error provides a further indication that a DNAPL source is still present in the second aquifer and may be located near the initial point of contamination, as suggested by previous papers that demonstrate the relative mobility of these sources (Luciano et al. 2010).

The second phase of the calibration procedure was aimed at determining the reactive transport with kinetic constants that described the abiotic dehydrochlorination of TeCA into TCE ($K_{\text{TeCA-TCE}}$). This abiotic dehydrochlorination is the only spontaneous transformation process likely to occur in a CAH-contaminated plume in the absence of an exogenous organic fermentable substrate, which could stimulate the biological activity of the dechlorinating biomass.

Data collected on the spatial and temporal (2003–2004) distribution of contaminants were used for the calibration phase. In order to estimate the most likely location and characteristics of the source, several simulations were conducted using different values for the TCE and TeCA concentrations

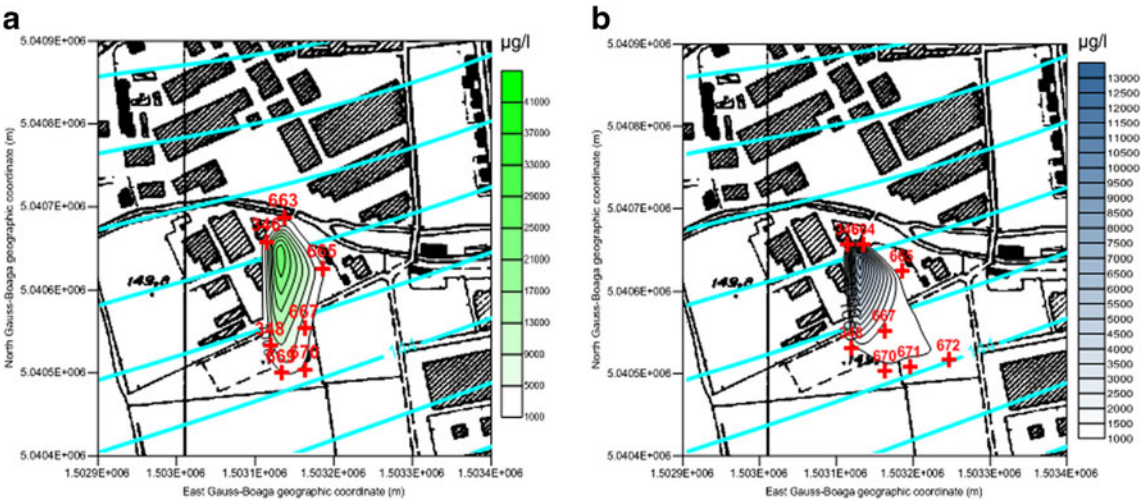

Fig. 5 Observed concentration on April 2004: **a** TCE and **b** TeCA

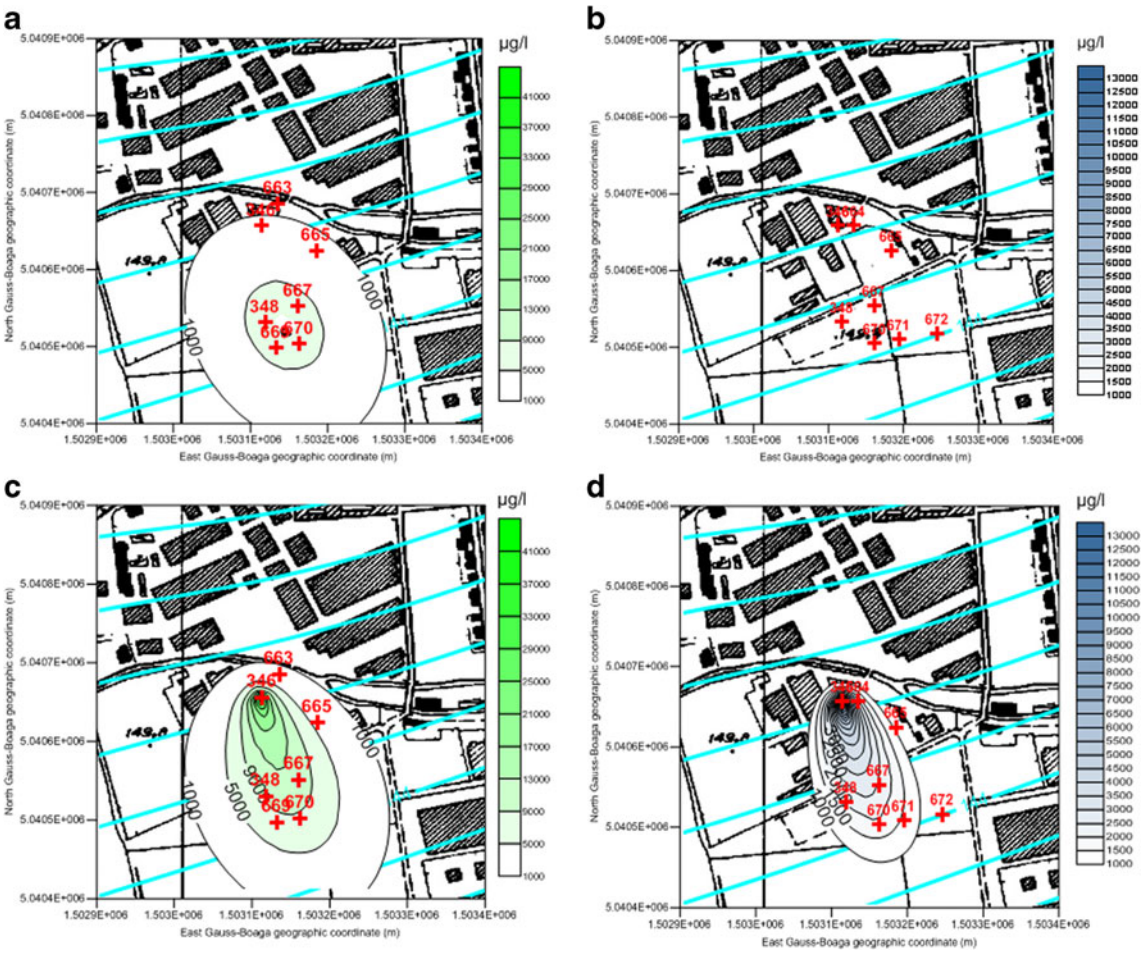

Fig. 6 Simulated concentrations: **a** TCE in the case of no-active contamination source; **b** TeCA in the case of no-active source; **c** TCE in the case of a persistent source in well 346 (325 µmol/L); and **d** TeCA in the case of a persistent source in well 346 (325 µmol/L)

with the assumption that the source was located near a predetermined well (346). The most suitable site, as reported in Fig. 7c, d, was the one with 325 (TCE) and 75 µmol/L (TeCA).

The following table (Table 2) reports the kinetic parameters used in the simulations (Bagley 1998; Fennell and Gossett 1998):

Forecast application of the model for ENA technology

After the calibration phase, a forecast analysis for an enhanced natural attenuation application was also performed. The reaction pathways assumed in the model are shown in Fig. 1. The choice to neglect the hydrogenolysis of TeCA (and of less-chlorinated ethanes) is partially justified by the fact that, at the site under investigation—given the long history of contamination (over 30 years)—abiotic dehydrochlorination was the main TeCA transformation step.

Lactate was chosen as a model electron donor based on the results of microcosm and pilot-scale tests (Aulenta et al. 2005a, b, 2006b, 2007). Indeed, the results from lactate-amended microcosms showed the shortest lag phase and the highest initial dechlorination rate. The concentrations of the different microbial populations that played a role in the complex biological processes, i.e., two classes of dechlorinators (X_{RD1} and X_{RD2}) and fermenters ($X_{Lat\text{-}Acet}$ and $X_{Lat\text{-}H2}$), were considered.

The results of the sensitivity analysis, not reported in this paper, indicate that the outcomes of the simulations were strongly dependent on the concentration of microorganisms thus making their quantification a crucial issue for both field studies and modeling efforts. Regardless, biomass values were set to constant because local changes were considered less important due to the long simulation times and the large heterogeneities of the soil. Under these conditions, model development on biomass concentrations would have been made fruitless because of uncertainties in the microbial/substrate spatial distribution and soil characteristics.

Regarding temporal changes in biomass concentration in remediation strategy design, the growth rates of various useful

species could make them unsuitable from an engineering point of view. Therefore, this model was used to evaluate the optimal biomass concentrations needed to reach the desired degradation ratio without a deeper discussion of the ways of reaching such concentrations.

The parameter values used in the simulations came from the literature, from laboratory tests (Aulenta et al. 2005a, 2006b) and from pilot-scale field tests (Aulenta et. al. 2005b, 2007). For a description of the results, four hypothetical monitoring points were used (P1, P2, P3, and P4). One of the reference points was located near the probable location of the source while the other three were located downgradient (Fig. 8).

Six scenarios based on various features (e.g., the amount of dechlorinating biomass, the amount of injected substrate, and the number and location of the injection points) with the same simulation time (5 years) were used to highlight the effects of different applications of the proposed technology on the results of enhanced natural attenuation as a GW remediation technology.

The different simulations are summarized in Table 3 shown below.

Application of the ENA in nonmodified conditions (case 1)

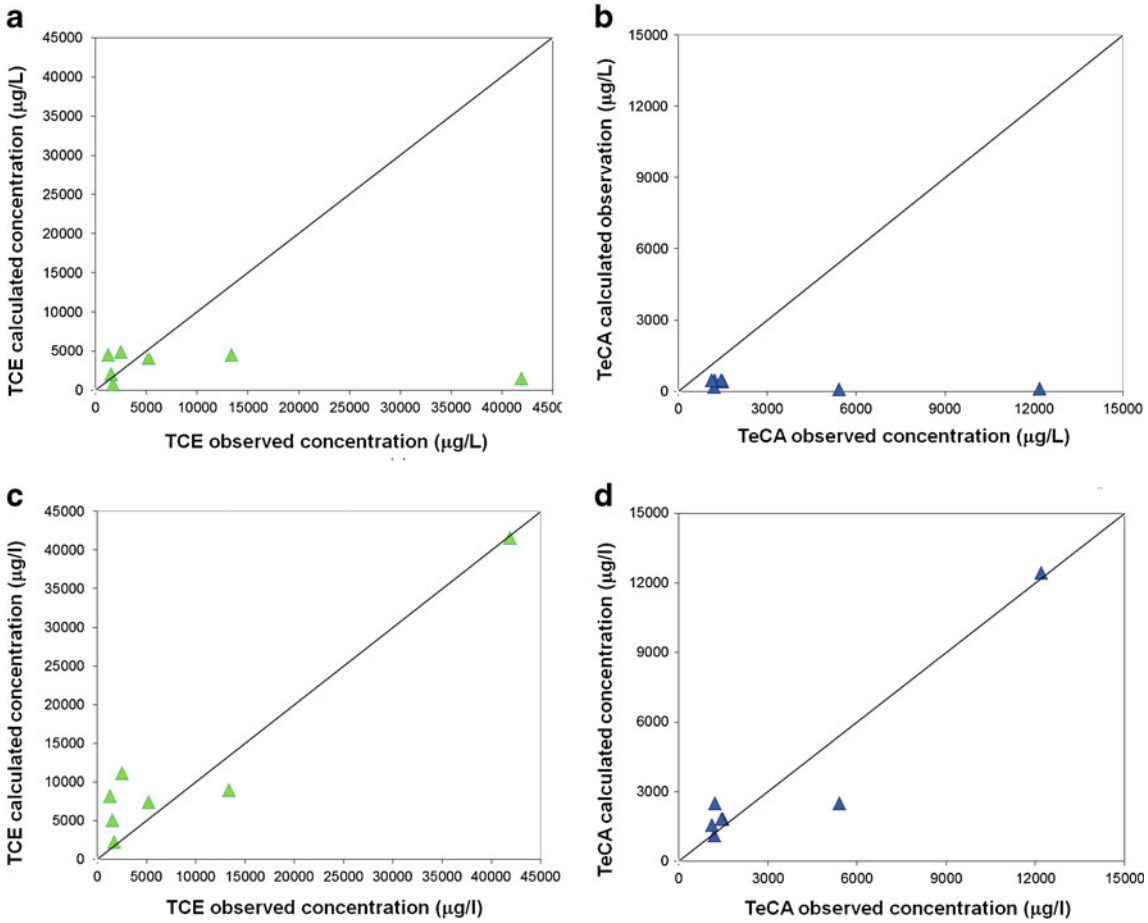

Fig. 7 Comparison between the observed and calculated concentrations: **a** TCE (eqm=61.52 %, no active source), **b** TeCA (eqm=53.31 %, no active source), **c** TCE (eqm=18.75 %, persistent source), and **d** TeCA (eqm=13.14 %, persistent source)

Figure 9a–d shows the simulation results for case 1. The behavior observed for both main contaminants (i.e., TCE and TeCA) in P1 (Fig. 9a) can be represented by a constant concentration due to their continuous release from the source. At other points (P2, P3, and P4), the TeCA concentration decreased (Fig. 9b–d). By contrast, TCE concentration at P2 and P3 exhibited an increasing phase followed by a decreasing phase (Fig. 9b, c), which can be attributed to the achievement of a steady state for the electron donor (H_2) and to the beginning of dechlorinating processes (ethene chain). In the last observation point (P4), only an increasing trend (Fig. 9d) was observed.

Breakdown product concentrations (DCE, VC, and ETH) showed a similar increasing trend at all observation points (Fig. 9a–d). For DCE, the highest value was found in P3 (4 µmol/L) at the end of the simulation (5 years). In P1 alone, a steady-state condition was observed at approximately halfway through the simulation, and this was followed by a slightly decreasing trend. For the VC compound, increasing values—from 0.2 µmol/L in P1 to 1.4 µmol/

Table 2 Kinetic parameters used for model simulations

Parameter	Values	Unit	References
Kinetic constants for RD			
$k_{TeCA\text{-}TCE}$	0.0001	μmol/mg VSS*h	Fixed
k_{TCE}	0.32	μmol/mg VSS*h	Tandoi et al. (1994)
$K_{S_{TCE}}$	2.16	μM	Smatlak et al. (1996)
k_{DCE}	0.236	μmol/mg VSS*h	Tandoi et al. (1994)
$K_{S_{DCE}}$	2.16	μM	Smatlak et al. (1996)
k_{VC}	0.197	μmol/mg VSS*h	Tandoi et al. (1994)
$K_{S_{VC}}$	3	μM	Balážová et al. (2006)
$K_{S_{H_2}}$	0.4	μM	Smatlak et al. (1996)
H_2th	0.3	nM	Löffler et al. (1999)
Dechlorinating biomass			
X_{RD1}	0.001	mg/L	Fixed
X_{RD2}	0.0005	mg/L	Fixed
Kinetic constants for fermentation (Fennell and Gossett)			
k_{latAc}	8.6	μmol/mg VSS*h	Fennell and Gossett (1998)
k_{latH_2}	8.6	μmol/mg VSS*h	Fennell and Gossett (1998)
K_{slatAc}	2.5	μM	Fennell and Gossett (1998)
$K_{S_{latH_2}}$	2.5	μM	Fennell and Gossett (1998)
K_{INL}	25	μmol/L	Fixed
Fermenting biomass			
X_{latAc}	0.1	mg/L	Fixed
X_{latH_2}	0.1	mg/L	Fixed

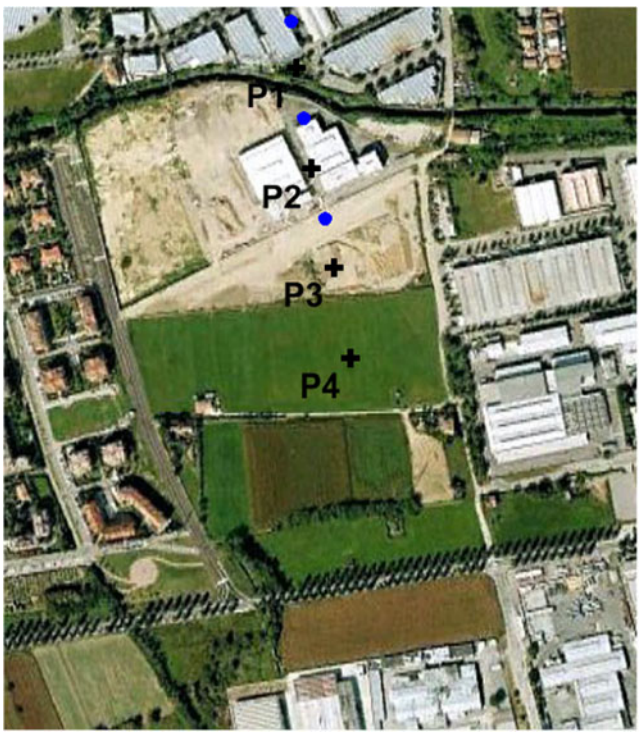

Fig. 8 Observation points

L in P4—were observed at all the observation points, whereas ethylene presents roughly the same values at all points (2.5–3.3 μmol/L), showing evidence of complete RD.

It is evident that, under these experimental conditions, enhanced bio-remediation is not suitable for reaching standard European limits in GW without the help of an intervention at the source. The following simulations provide definitive evidence in support of this finding.

Source removed—application of ENA (cases 2–6)

Variations in percent ratios for all contaminants and their breakdown products at the first (P1) and last (P4) monitoring points are listed in Table 4.

As breakdown product concentrations increased during each simulation, none of the primary contaminants reached the limits for GW required by Italian law (D.Lgs. 152/2006). Moreover, the concentrations of some breakdown products, especially DCE and VC (which are more toxic than TCE and TeCA), highlight a major risk associated with the use of a hardly controllable remediation technology that is capable of producing compounds that are more dangerous than the initial contaminants. The recalcitrance of these breakdown products is linked to the fact that chlorinated compounds with fewer chlorine atoms are degraded with more difficulty by anaerobic processes than are TeCA or TCE.

Figure 10 shows the trends of all contaminants for the 4th simulation at each observation point. These results were obtained by increasing the dechlorinating biomass at the site. Biostimulation, by the addition of the eletron donor, represents one of the most effective approaches for achieving the desired degradation rates, especially considering the important kinetic parameters used in the model, as listed in Table 5. The assigned values represent the maximum ones that can be set for biomass concentrations (Clapp et al. 2004). The biomass concentrations were augmented equally in each simulation to avoid an imbalance in the RD process.

These results indicate that the biomass concentrations caused faster degradation of TCE and TeCA, coupled with greater development of breakdown products, and thus achieved complete removal in P1.

By an analysis of trends at the observation points (P2, P3, and P4), as seen in Fig. 10, it is possible to discern an incomplete RD process despite greater degradation of the primary contaminants and increases in DCE, VC, and ETH, as predicted from the equations describing the process.

A further intervention could be made by enhancing the lactate concentration to stimulate electron donor (H_2, 2 g/L—5th case) availability. However, our results do not encourage this solution due to limitations that result in removal percentages similar to those of the second case.

Table 3 Features of different simulations

Case	Case 1	Case 2	Case 3	Case 4	Case 5	Case 6
Source	TCE, 325 μmol/L TeCA, 70 μmol/L in 346 well	Removed	Removed	Removed	Removed	Removed
Dechlorinating biomass	Calibration condition	Calibration condition	Decreased one order of magnitude	Increased one order of magnitude	Calibration condition	Calibration condition
Injection of substrate	1 point in 346 well	1 point in 346 well	1 point in 346 well	1 point in 346 well	1 point in 346 well	3 points offset downgradient
Substrate concentration injection	1 g/L	1 g/L	1 g/L	1 g/L	2 g/L	1 g/L
Simulation time	5 years	5 years	5 years	5 years	5 years	5 years

As in case 5, the last simulation can be considered a further test to evaluate whether a different lactate release could improve the electron donor spatial distribution and consequently accelerate the RD process. Three lactate injection

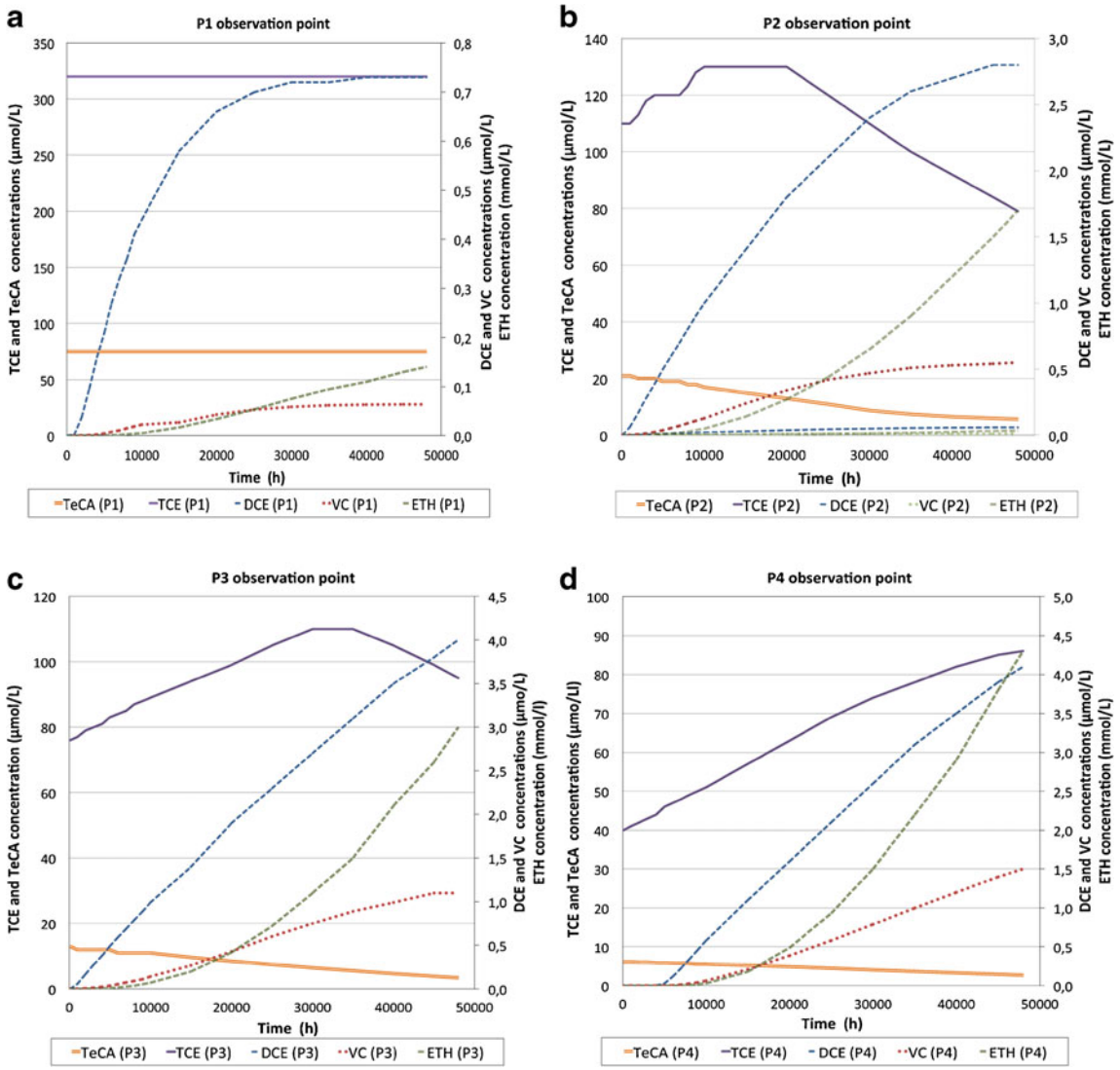

Fig. 9 Calculated concentrations over time in P1 (**a**), in P2 (**b**), in P3 (**c**), and in P4 (**d**)

Table 4 Percent reaction in P4 (final concentrations) compared with P1 (initial concentrations; TeCA data include only abiotic transformation)

Product	Simulation 2 reaction (%)	Simulation 3 reaction (%)	Simulation 4 reaction (%)	Simulation 5 reaction (%)	Simulation 6 reaction (%)
TCE	−68	−67	−81	−68	−68
TeCA	−96	−96	−96	−96	−96
DCE	640	727	551	640	720
VC	4.186	7.461	1.463	4.067	4.111
ETH	38.610	85.614	4.567	41.835	48.385
H_2	509	639	65	1.103	3.693

points were chosen, spaced 50 m apart and parallel to the GW flow, starting upstream of the P1 observation point as shown in Fig. 8 (indicated by blue points).

In this case, even if the H_2 concentration increased to a high value, as shown in Fig. 11c, an enhancement in the RD process was not observed. Thus, it would be much more effective to limit lactate injection quantity and to find the best injection sites to produce an optimal distribution in the GW.

From the reported results it stems that the option to use ENA for the GW treatment, with the dechlorination process as active de-contaminators, cannot bring to contaminants concentrations lower than law limit, even with ammendants injection, without a drastic intervention on the long-term source. Furthermore, the long-time need to allow biomass development for a complete RD processes indicates that ENA Technology is not suitable in this site.

Conclusions

The proposed model validated in this study has allowed the simulation of several scenarios that can be used for the optimization of the remediation technology in every important aspect (e.g., the positions of the injection points, the quantity and concentration of substrates, the monitoring wells, and the expected remediation limit). The fundamental outcomes of

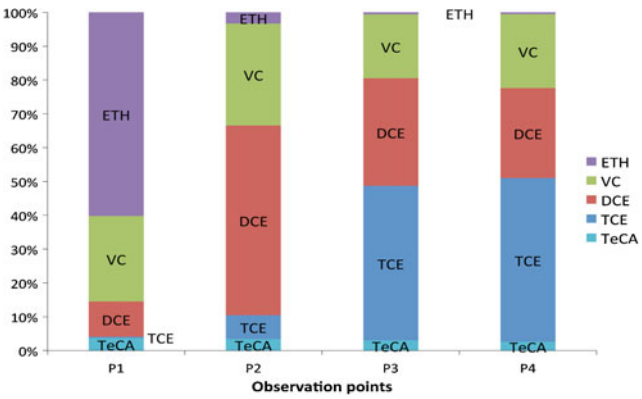

Fig. 10 Calculated concentrations at the end of simulation 4

Table 5 Dechlorinating biomass

Parameter	Values	Unit	References
X_{RD1}	0.01	mg/L	Fixed
X_{RD2}	0.005	mg/L	Fixed
Biomass concentration (fermentation phase)			
X_{latAc}	0.5	mg/L	Fixed
X_{latH_2}	0.5	mg/L	Fixed

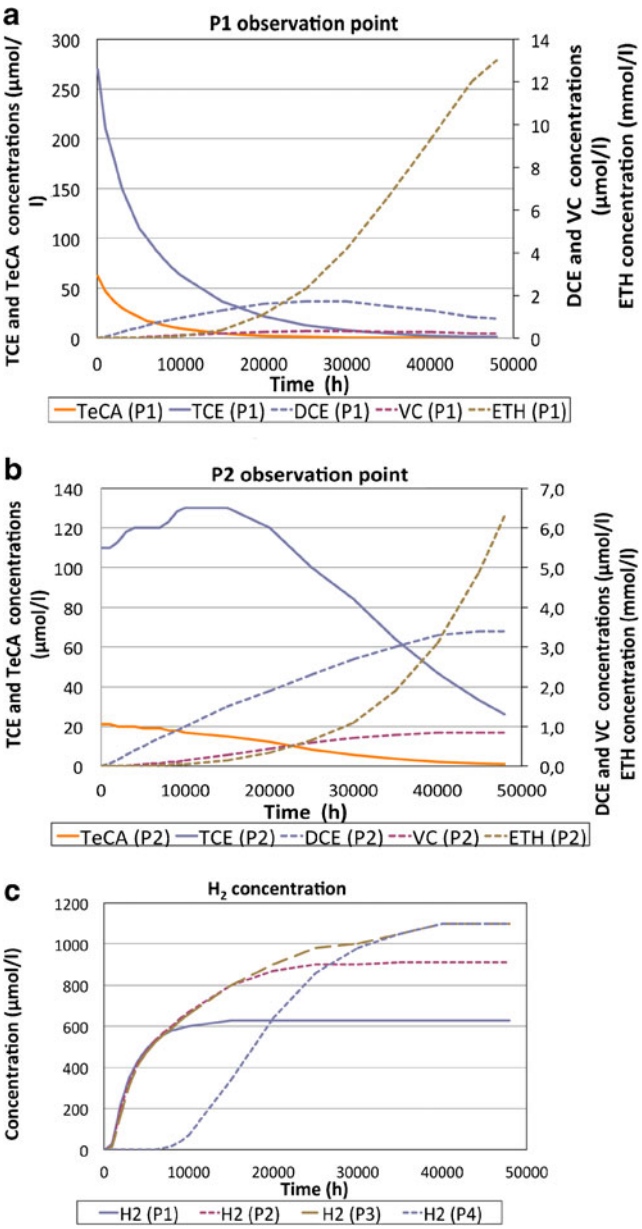

Fig. 11 Calculated concentrations vs. time in P1 (**a**), in P2 (**b**), and in all observation points (**c**)

the numerical model was surely the possibility of defining the existence of a long-term contamination source in the deep aquifer and its probable position, furthermore to verify, thanks to the complete pathway that can be forecasted by means numerical simulations, an optimal use of eventual ammendants and of their distribution technology for the application of the ENA Technology.

The primary issues for the modeling phase are the lack of information on kinetics, the need to verify the presence of biomass suitable for the dechlorinating processes, and the need to carry out laboratory tests to analyze the possibility of divergent reactive pathways in the presence of competitors. Moreover, a future implementation of the model could involve varying the concentration of the injected biomass and its distribution to study the development of the dechlorinating processes in space and time.

It is evident that enhanced natural attenuation technology needs a comprehensive approach to ensure that the remediation of a contaminated plume happens as expected. It is also clear that source removal is necessary to achieve the required reductions in GW contaminant concentrations. Thus, the ENA approach to remediating an existing mobile plume can only be useful if coupled with an intervention to physically remove the source of the released substances.

A better characterization of the source (e.g., multiple microglobules vs. a single DNAPL pool) would allow one to conduct more targeted experiments, such as injecting biomass or substrate directly into the source areas or mobilizing the source by creating an artificial hydraulic gradient. These two experiments could help verify the processes of mass reduction due to the initial contaminant distribution (Luciano et al. 2012) and the degradative effects of biomass action.

Moreover, an effective amendment distribution is necessary to optimize electron donor (H_2) development for the RD process. Active biomass levels responsible for dechlorination (*Dehaloccoides* spp.) in the field are difficult to determine; consequently, the quantities of substrate necessary to stimulate bacterial activity must be estimated with numerical simulations.

The real limit of ENA technology, especially in urbanized areas, is a lengthy remediation time due to the slow rates of biological reactions. Furthermore, a great risk lies in the possibility that contaminant concentrations will not reach the legal limits mandated for GW quality.

The results from the experimental scenarios show that augmenting the injected substrate quantity or the number of injection points does not necessarily produce significant changes in the degradation efficiency. These results can be predicted from an analysis of the dechlorination process kinetics.

The availability of a numerical code that is able to simulate the effects of different scenarios, and which can be used to design a better substrate feed system to bolster the degradation process, will enhance the effectiveness of inexpensive ENA Technology.

Acknowledgment This research was financially supported by the European Union (European Commission, FP7 contract no. 213161).

References

Aulenta F, Bianchi A, Majone M, Petrangeli Papini M, Potalivo M, Tandoi V (2005a) Assessment of natural or enhanced in situ bioremediation at a chlorinated solvent-contaminated aquifer in Italy: a microcosm study. Environ Int 31:185–190

Aulenta F, Di Fazio A, Leccese M, Majone M, Petrangeli Papini M, Rossetti S, Stracqualursi N, Tandoi V, Viotti P (2005) Assessing the potential for natural or enhanced in-situ bioremediation at a TCE-contaminated site by coupling process analysis and modeling. In: Nutzmann G, Viotti P, Aagaard P (eds) Reactive transport in soil and groundwater. Springer, Berlin, pp. 165–177

Aulenta F, Potalivo M, Majone M, Petrangeli Papini M, Tandoi V (2006a) Anaerobic bioremediation of groundwater containing a mixture of 1,1,2,2-tetrachloroethane and chloroethenes. Biodegradation 17(3):193–206

Aulenta F, Pera A, Rossetti S, Petrangeli Papini M, Majone M (2006b) Relevance of side reactions in anaerobic reductive dechlorination microcosms amended with different electron donors. Water Res 41:27–38

Aulenta F, Canosa A, Leccese M, Petrangeli Papini M, Majone M, Viotti P (2007) Field study of in situ anaerobic bioremediation of a chlorinated solvent source zone. Ind Eng Chem Res 46(21):6812–6819

Bagley DM (1998) Systematic approach for modelling tethrachloroethene biodegradation. J Environ Eng-Asce 124:1076–1086

Balážová A, Slodička M, Van Keer R (2006) Parameter determination for reductive dechlorination of chlorinated solvents. Transp Porous Media 65:411–424

Beretta GP, Bozzano F, Del Bon A, Majone M, Nardoni F, Pacioni E, Petitta M, Viotti P (2006) Multi-scale approach for geological and hydrogeological characterization of a polluted site in the municipality of Rho (MI). In: Proceedings International Conference on the Remediation of Polluted Sites BOSICON, Rome, (CD-Rom)

Boulding RJ. Ginn JS (2004) Practical handbook of soil, vadose zone, and ground-water contamination: assessment, prevention, and remediation

Bozzano F, Petitta M, Del Bon A, Nardoni F, Pacioni E (2007) Conceptual model and flow numerical simulation of aquifer contaminated by chlorinated solvents in Rho (MI). Ital J Eng Geologi Enviroment Spec Issue 1:97–105

Clapp LW, Semment MJ, Novak PJ, Hozalski RM (2004) Model for in situ perchloroethene dechlorination via membrane-delivered hydrogen. J Environ Eng-ASCE 130(11):1367–1381

Clement PT, Johnson CD, Sun Y, Klecka GM, Bartlett C (1998) Natural attenuation of chlorinated ethane compounds: model development and field-scale application at the Dover site. J Cont Hydrol 42:113–140

Clement PT, Truex MJ, Lee P (2001) A case study for demonstrating the application of U.S. EPA's monitored natural attenuation screening protocol at a hazardous waste site. J Cont Hydrol 59:133–162

Fennel DE, Gosset JM (2003) Microcosms for site specific evaluation of enhanced biological reductive dehalogenation. In: Häggblom, M.H. Bossert ID (eds) Dehalogenation: microbial processes and environmental applications. Kluwer Academic Publisher, Amsterdam, pp. 1–11

Fennell DE, Gossett JM (1998) Modeling the production of and competition for hydrogen in a dechlorinating culture. Environ Sci Technol 32:2450–2460

Fennell DE, Carroll AB, Gossett JM, Zinder SH (2001) Assessment of indigenous reductive dechlorinating potential at a TCE-contaminated site using microcosm, polymerase chain reaction analysis, and site data. Environ Sci Technol 35:1830–1839

Grostern A, Edwards EA (2006) Growth of Dehalobacter and Dehalococcoides spp. during degradation of chlorinated ethanes. Appl Environ Microb 72(1):428–436

Harbaugh AW, Banta ER, Hill MC, McDonald MG (2000) MODFLOW-2000, the U.S. Geological Survey modular groundwater model. User guide to modularization concepts and the ground-water flow processes. U.S. Geological Survey Open-File Report 00–92, 121. USGS, Reston

Kuchovsky T, Sracek O (2007) Natural attenuation of chlorinated solvents: a comparative study. Environ Geol 53:147–157

Löffler FE, Tiedje JM, Sanford RA (1999) Fraction of electrons consumed in electron acceptor reduction and hydrogen thresholds as indicators of halorespiratory physiology. Appl Environ Microb 65(9):4049–4056

Logan BE, Sang-Eun O, In SK, Van Ginkel S (2002) Biological hydrogen production measured in batch anaerobic respirometers. Environ Sci Technol 36(11):2530–2535

Lorah MM, Voytek MA (2002) Degradation of 1,1,2,2-tetrachloroethane and accumulation of vinyl chloride in wetland sediment microcosms and in situ porewater: biogeochemical controls and associations with microbial communities. J Cont Hydrol 70:117–145

Luciano A, Petrangeli Papini M, Viotti P (2010) Laboratory investigation of DNAPL migration in porous media. J Hazard Mater 176:1006–1017

Luciano A, Viotti P, Petrangeli Papini M (2012) On morphometric properties of DNAPL sources: relating architecture to mass reduction. Water Air Soil Poll 223(5):2849–2864

Nobre RC, Nobre MM (2004) Natural attenuation of chlorinated organics in a shallow sand aquifer. J Hazard Mater 110:129–137

Rivett MO, Feenstra S, Cheny JA (2001) A controlled field experiment on groundwater contamination by a multicomponent DNAPL: creation of the emplaced-source and overview of dissolved plume development. J Cont Hydrol 49(1–2):111–149

Roy JW, Smith JE, Gilham RW (2002) Natural remobilization of multicomponent DNAPL pools due to dissolution. J Cont Hydrol 59(3–4):163–186

Rossetti S, Aulenta F, Majone M, Crocetti G, Tandoi V (2008) Structure analysis and performance of a microbial community from a contaminated aquifer involved in the complete reductive dechlorination of 1, 1, 2, 2-tetrachloroethane to ethene. Biotechnol Bioeng 100(2):240–249

Smatlak CR, Gossett JM, Zinder SH (1996) Comparative kinetics of hydrogen utilization for reductive dechlorination of tetrachloroethene and methanogenesis in an anaerobic enrichment culture. Environ Sci Technol 30:2850–2858

Suthersan S (2002) Natural and Enhanced Remediation Systems. Lewis Publishers

Tandoi V, Di Stefano T, Bowser P, Gosset JM, Zinder SH (1994) Reductive dehalogenation of chlorinated ethenes and halogenated ethanes by a high rate anaerobic enrichment culture. Environ Sci Technol 28:973–979

Tosco T, Bosch J, Meckenstock R, Sethi R (2012) Transport of ferrihydrite nanoparticles in saturated porous media: role of ionic strength and flow rate. Environ Sci Technol 46:4008–4015

Wiedemeier TH, Rifai HS, Newell CJ, Wilson JT (1999) Natural attenuation of fuels and chlorinated solvents in the subsurface. Wiley, New York

Witt ME, Klecka GM, Lutz EJ, Ei TA, Grosso NR, Chapelle FH (2000) Natural attenuation of chlorinated solvents at Area 6, Dover Air Force Base: groundwater biogeochemistry. J Cont Hydrol 57:61–80

Wood RC (2005) Modeling application of hydrogen release compound to effect in situ bioremediation of chlorinated solvent-contaminated groundwater. Thesis Air Force Institute of Technology

Yu S, Dolan ME, Semprini L (2005) Kinetics and inhibition of reductive dechlorination of chlorinated ethylenes by two different mixed cultures. Environ Sci Technol 39(1):195–205